This article has been published in: Acta Biomaterialia 2018 Mar 24. pii: S1742-7061(18)30164-8. doi:10.1016/j.actbio.2018.03.033.

Graphical Abstract

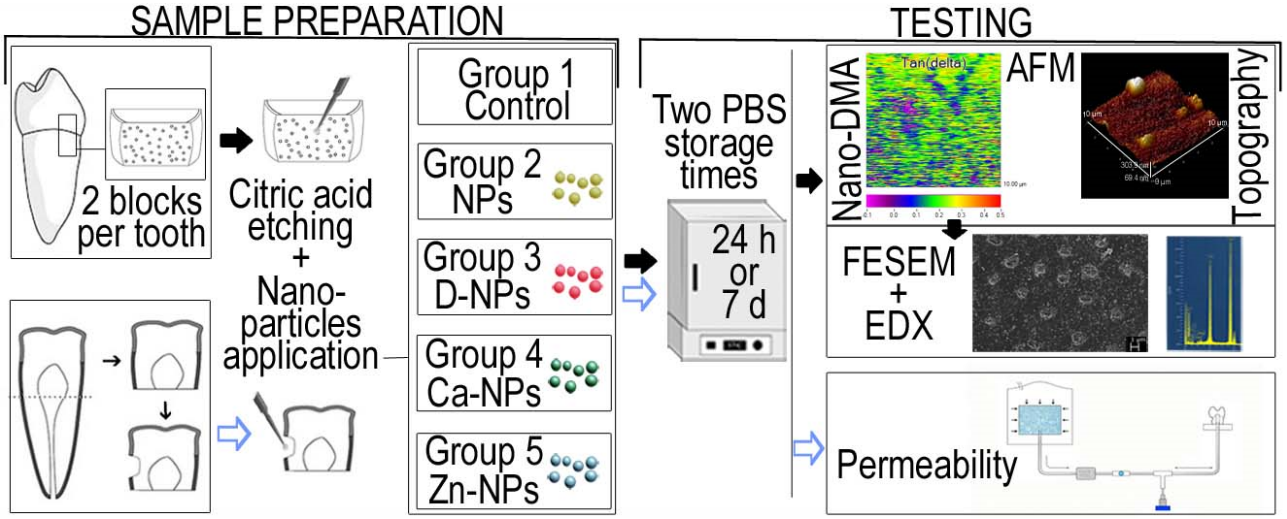

Statement of significance

Erosion from acids provokes dentin hypersensitivity (DH) which presents with intense pain of short duration. Open dentinal tubules and demineralization favor DH. Nanogels based on Ca-nanoparticles and Zn-nanoparticles produced an efficient reduction of fluid flow. Dentinal tubules were filled by precipitation of induced calcium-phosphate deposits. When treating dentin with Zn-nanoparticles, complex modulus values attained at intertubular and peritubular dentin were higher than those obtained after applying Ca-nanoparticles. Zn-nanoparticles are then supposed to fasten active dentin remodeling, with increased maturity and high mechanical properties. Zinc-based nanogels are, therefore, proposed for effective dentin remineralization and tubular occlusion. Further research to finally prove for clinical benefits in patients with dentin hypersensitivity using Zn-doped nanogels is encouraged.

Title: Improved reactive nanoparticles to treat dentin hypersensitivity.

Running title: Nanoparticles for treating dentin hypersensitivity.

Authors: Manuel Toledano-Osorio[a], Estrella Osorio[a], Fátima S. Aguilera[a], Antonio Luis Medina-Castillo[b], Manuel Toledano[a*], Raquel Osorio[a].

Institution: [a]University of Granada, Faculty of Dentistry, Dental Materials Section.
Colegio Máximo de Cartuja s/n
18071 – Granada - Spain.

[b]University of Granada, NanoMyP. Spin-Off Enterprise.
Edificio BIC-Granada. Av. Innovación 1.
18016 - Armilla, Granada, Spain.

*Corresponding author: Prof. Manuel Toledano.
University of Granada, Faculty of Dentistry
Dental Materials Section
Colegio Máximo de Cartuja s/n
18071 – Granada - Spain.
Tel.: +34-958243788
Fax: +34-958240809
Email: toledano@ugr.es

ABSTRACT

The aim of this study was to evaluate the effectiveness of different nanoparticles-based solutions for dentin permeability reduction and to determine the viscoelastic performance of cervical dentin after their application. Four experimental nanoparticle solutions based on zinc, calcium or doxycycline-loaded polymeric nanoparticles (NPs) were applied on citric acid etched dentin, to facilitate the occlusion and the reduction of the fluid flow at the dentinal tubules. After 24 h and 7 d of storage, cervical dentin was evaluated for fluid filtration. Field emission scanning electron microscopy, energy dispersive analysis, AFM and Nano-DMA analysis were also performed. Complex, storage, loss modulus and tan delta (δ) were assessed. Doxycycline-loaded NPs impaired tubule occlusion and fluid flow reduction trough dentin. Tubules were 100% occluded in dentin treated with calcium-loaded NPs or zinc-loaded NPs, analyzed at 7 d. Dentin treated with both zinc-NPs and calcium-NPs attained the highest reduction of dentinal fluid flow. Moreover, when treating dentin with zinc-NPs, complex modulus values attained at intertubular and peritubular dentin were higher than those obtained after applying calcium-NPs. Zinc-NPs are then supposed to fasten active dentin remodeling, with increased maturity and high mechanical properties. Zinc-based nanoparticles are then proposed for effective dentin remineralization and tubular occlusion. Further research to finally prove for clinical benefits in patients with dentin hypersensitivity using Zn-doped nanoparticles is encouraged.

Key words: cervical dentin, hypersensitivity, DMA, nanoparticles

1. Introduction

As the prevalence of both caries and periodontal disease has declined because of oral health promotion strategies, other pathologies as dentin hypersensitivity (DH) have come to the forefront. Dentin is the composite mineralized tissue with mechanical properties essential to protect enamel, maintaining the stress/strain tooth behavior. It is crossed by the dentinal tubules. Each tubule lumen is surrounded by a peritubular cuff, which consists of a hyper-mineralized collagen-poor region of apatite crystals [1]. They are oriented radially from the pulp toward the dentin-enamel junction, and in DH they are in close proximity to each other [2]. Intertubular dentin occupies the region between the tubules and consists of an organic matrix (collagen fibrils) reinforced by nanoscopic apatite crystals similar to that of peritubular dentin [3].

DH is clinically described as a non-spontaneous, localized, intense pain of short duration that ceases when stimuli are removed [4]. Erosion has been considered the main etiological factor for DH, because it is capable of opening and enlarging the dentin tubules [2]. Open dentinal tubules allow fluid flow through the tubules, which results in pressure changes that excite the nerve ending in the dental pulp [5]. The occlusion of dentinal tubules, therefore, is considered one of the main objectives of DH therapy [6,7]. Desensitizing products including varnishes, resins and remineralizing agents have been proposed for tubule occlusion, but with uncertain results [7]. Nanoparticles are 100-nm crosslinked globular particles synthesized through a versatile route with methacrylate functionalization. Nanoparticles, in dentin treatment, are anticipated to carry the nanoparticles (NPs) into demineralized dentin [8]. Dentin infiltration with polymeric NPs as calcium and phosphate sequestering materials (i.e, carboxylate-functionalized polymer particles) has been proposed [9]. These polymers should bind to collagen and facilitate the formation of amorphous calcium/phosphate precursors for dentin remineralization

[10]. There are evidences of the bioactivity of NPs in apatite formation, which may be crucial in treating DH by remineralization effects. Nanopolymers may also act as carriers of other biological factors for the management of tissue mineralization. Zinc can also be quelated at these particles in order to inhibit collagen degradation and stimulate dentin remineralization [11]. The formula for stoichiometric HAp is $Ca_{10}(PO_4)_6(OH)_2$. An isomorphous substitution can be obtained when Ca^{2+} is replaced by Zn^{2+} into dentin HAp [12]. At the intertubular dentin, remaining collagen (if denatured) is susceptible to degradation by host-derived matrix metalloproteinases [13]. Doxycycline is not only an antibacterial but also is known to provoke a potent and long-lasting inhibition of dentin matrix metalloproteinases (MMPs) [14]. As MMPs are related with the progression of eroded lesions at cervical dentin [15], it would be desirable to introduce this compound for eroded lesions at cervical dentin. However, it should be demonstrated that it will not affect dentin remineralization. It should be taken into account that doxycycline has been shown to initiate demineralization on dentin surface layers, and may trigger mineralization [16,17].

Viscoelastic materials located at load-bearing areas, such as dentin [18] exhibit time-dependent strain [19,20]. Therefore, it is of interest to examine, with nano-dynamic mechanical analysis (nano-DMA) [21], both the complex modulus (E^*) and damping or tan delta (δ) of these treated cervical dentin surfaces [22]. The aim of this study was to evaluate the ability to occlude the patent dentinal tubules measuring its effect on conductance across the dentin, and to study the viscoelastic behavior of cervical dentin surfaces treated with four different nanoparticles-based solutions for remineralizing purposes. The null hypotheses tested were as follows: (1) the application of NPs loaded with doxycycline, zinc or calcium onto exposed cervical dentin would not promote the occlusion of dentinal tubules and the reduction of hydraulic conductance, and (2) the

application of NPs loaded with doxycycline, zinc or calcium onto cervical dentin would not produce changes on viscoelasticity.

2. Materials and Methods

2.1. Nanoparticles production

PolymP-*n* Active nanoparticles (NPs) (NanoMyP, Granada, Spain) were fabricated trough polymerization precipitation [23]. NPs are composed by 2-hydroxyethyl methacrylate (backbone monomer), ethylene glycol dimethacrylate (cross-linker) and methacrylic acid (functional monomer). Calcium-doped NPs (Ca-NPs) and Zinc-doped NPs (Zn-NPs) were produced. For zinc and calcium complexation 30 mg of NPs were immersed at room temperature, during 3 days under continuous shaking in 15 ml aqueous solutions of $ZnCl_2$ or $CaCl_2$ (containing zinc or calcium at 40 ppm at pH 6.5), in order to reach the adsorption equilibrium of metal ions [9]. Then, the suspensions were centrifuged (7,800 rpm/G-force=6,461) during 20 min and the particles were separated from the supernatant. Same centrifugation procedure was repeated twice, adding PBS solution for washing purposes. Attained ion complexation values were 0.96 ± 0.04 μg Ca/mg NPs and 2.15 ± 0.05 μg Zn/mg NPs [24]. A third group of NPs doped with doxycycline was introduced in the study. 30 mg of NPs were immersed in 18 ml of 40 mg/ml aqueous solution of doxycycline hyclate (Sigma Aldrich, ChemieGmbh, Riedstr, Germany), during 4 hours, under continuous shaking. Then, the suspensions were centrifuged (7,800 rpm/G-force=6,461) during 20 min and the particles were separated from the supernatant and washed as described above. In each mg of NPs, 933 μg Dox/mL were loaded [25]. The size of NPs did not change after loading, and no agglomeration was produced. Hydrodynamic size distribution of nanoparticles was assessed by dynamic light scattering (DLS) (Zetasizer™ v. 7.11, Malvern Instruments™) in deionized water.

Average size and standard deviations using DLS analysis were: NPs 250.10±7.46 nm, D-NPs 244.36±9.79 nm, Zn-NPs 225.93±8.88 nm and Ca-NPs 238.10±10.96.

Four different nanoparticles solutions were produced suspending NPs in PBS solutions at a concentration of 10mg/ml: 1) NPs (NPs), 2) NPs doped with Ca (Ca-NPs), 3) NPs doped with Zn (Zn-NPs), and 4) NPs doped with doxycycline hyclate (D-NPs).

2.2. Dentin Permeability Evaluation

Thirty sound single-rooted teeth were obtained with informed consent from donors (18 to 25 yr of age), under a protocol approved by the Institution review board (#405/CEIH/2017). Each root was removed 5 mm below the cement-enamel junction using a low-speed diamond saw (Accutom-50 Struers, Copenhagen, Denmark). The pulp tissue in the pulp chamber was carefully removed without altering the pre-dentin surface using thin tissue forceps and endodontic files. A sand-blasted plexiglass square with a hole drilled at its center was used to mount each tooth in the fluid filtration system. A metal tube with a diameter of 0.9 mm was inserted into the hole, and the plexiglass was attached to the tooth using an adhesive (Adper Scotchbond MultiPurpose, 3M ESPE, St Paul, MN, USA) and a resin composite (TetricEvoCeram R, Ivoclar Vivadent, Schaan, Liechtenstein), to ensure that one end of the metal tube was located in the pulp chamber. Interconnections were covered with nail varnish. The rest of the procedure was as in Kim et al., 2013 [26].

A V-shaped cervical cavity with a mesial-distal width of 5 mm, and occluso-cervical height of 3 mm, and a depth of 2 mm was prepared with a 801-014 carbide bur (diamond bur of ≈ 107 μm grit size). Acid etching (32% phosphoric acid) was performed to remove the smear layer. The cavity was then rinsed with water and blot-dried with a wet cotton pellet. The measurement of the fluid volume through the sensor was

performed. The highest hydraulic conductance for each specimen after phosphoric acid treatment was recorded (P_{max}). A PBS suspension of NPs, Zn-NPs, Ca-NPs, D-NPs (10 mg/ml) or just PBS solution were applied (30 s), in each of the five different experimental groups. Specimens were connected to a hydraulic pressure device with a liquid flow sensor (ASL 1600, Sensirion, Staefa, Switzerland). A constant hydraulic pressure of 6.9 kPa was applied [26] to simulate physiological pulp pressure [26,27] (Fig 1a).

Dentin permeability was calculated after nanoparticles application and artificial PBS storage for 24 h and 7 d. The dentinal fluid flow (DFF) through the cervical dentin was measured at these time points. Five fluid volume readings were recorded every 3 min during 15 min and the average calculated. The average DFF, as measured before the NPs placement was set as the baseline flow rate. It was assessed the DFF rate after the agents application, with respect to the baseline flow rate [% reduction in flow rate = 100 x (flow $rate_{baseline}$ - flow $rate_{postapplication}$)/flow $rate_{baseline}$] [26].

2.3. Nano-DMA and Atomic Force Microscopy (AFM) analyses

Further 15 sound, single-rooted teeth were obtained with informed consent from donors (18 to 25 yr of age), under a protocol approved by the Institution review board (#405/CEIH/2017). From each tooth, two dentin blocks were obtained from the buccal surface of the root, just below the cementodentinal junction. The tooth was cut perpendicular to the axial axis using a diamond saw (Accutom-50 Struers, Copenhagen, Denmark) under copious water irrigation to obtain cementodentinal slabs with a thickness of 1 mm. The surfaces were polished through SiC abrasive papers from 800 up to 4000 grit followed by final polishing steps performed using diamond pastes through 1 μm down to 0.25 μm (Struers LaboPol-4; Struers GmbH, Hannover, Germany) (Fig 1b). The specimens were treated in ultrasonic bath (Model QS3, Ultrawave Ltd, Cardiff, UK)

containing deionized water for 5 min at each polishing step. The specimens were finally stored in buffered deionized water [pH: 7.1] for no more than 12 h. Specimens were prescreened for tubule occlusion with AFM (AFM Nanoscope V, Digital Instruments, Veeco Metrology group, Santa Barbara, CA, USA) and those with occluded tubules were excluded. Tubules were exposed by dipping the dentin samples into a citric acid solution (pH 3.8) for 1 min to ensure the patency of the dentinal tubules and remove the smear layer. Dentin surfaces were washed and ultrasound treated for 10 min before NPs application [28]. A PBS suspension of NPs, Zn-NPs, Ca-NPs, D-NPs (10 mg/ml) or just a PBS solution were applied (30 s), in each of the five different experimental groups. Specimens were tested after storing in PBS at 37o C for 24 hours and 7 days.

Three blocks of each treated dentin were subjected to nano-DMA and AFM analyses. Nanomechanical properties were assessed by means of a Hysitron Ti Premier nanoindenter (Hysitron, Inc., Minneapolis, MN), a commercial nano-DMA package. The nanoindenter tip was calibrated against a fused quartz sample using a quasistatic force setpoint of 2 μN to maintain contact between the tip and the sample surface. A dynamic (oscillatory) force of 2 μN was superimposed on the quasistatic signal at a frequency of 200 Hz. Based on a calibration-reduced modulus value of 69.6 GPa for the fused quartz, the best-fit spherical radius approximation for tip was found to be 85 nm, for the selected nano-DMA scanning parameters. Modulus mapping of our samples was conducted by imposing a quasistatic force setpoint, Fq=2 μN, to which we superimposed a sinusoidal force of amplitude FA=0.10 μN and frequency f=100 Hz. The resulting displacement (deformation) at the site of indentation was monitored as a function of time. Data from regions approximately 10×10 μm in size were collected using a scanning frequency of 0.2 Hz [29]. Specimens were scanned under a hydrated condition. In order to accomplish for this purpose, samples were stored in PBS after polishing to maintain the hydration.

Prior to the nanomechanical experiment, samples were removed from the hydration bath and the excess PBS was wiped away. To maintain the hydration of dentin samples while eliminating problems related to the meniscus forces transferred from droplets of fluid to the indenter [29], a drop (1.5 ml) of 99.4% ethylene glycol was applied to the polished sample surface [30]. Under steady conditions (application of a quasistatic force) the indentation modulus of the tested sample, E, can be obtained by application of different models that relate the indentation force, F, and depth, D [31]. Three modulus mapping were taken on each dentin surface. From each mapping 15 value points of complex modulus, loss modulus, storage modulus, tan and stiffness were recorded for each type of dentin (peritubular or intertubular).

An atomic force microscope (AFM Nanoscope V, Digital Instruments, Veeco Metrology group, Santa Barbara, CA, USA) was employed in this study for topography mappings. The imaging process was undertaken inside a fluids cell of the AFM in a fully hydrated state, using the tapping mode, with a calibrated vertical-engaged piezo-scanner (Digital Instrument, Santa Barbara, CA, USA). A 10 nm radius silicon nitride tip (Veeco) was attached to the end of an oscillating cantilever (spring constant: 20 to 80 N/m) that came into intermittent contact with the surface at the lowest point of the oscillation. The fluid holders were designed to allow the laser light to be reflected on the cantilever in solution, while keeping the scanner tube to come into contact with the fluid environment. Changes in vertical position of the AFM tip at resonance frequencies near 330 kHz provided the height of the images registered as bright and dark regions. 10 x 10 μm digital images were recorded from each dentin surface, with a slow scan rate (0.1 Hz).

2.4. Field Emission Scanning Electron Microscopy (FESEM) and energy dispersive (FESEM/EDX) analyses

After nano-DMA and AFM analysis, specimens were fixed in a solution of 2.5% glutaraldehyde in 0.1 mol/L sodium cacodylate buffer for 24 h. Samples were subjected to critical point drying (Leica EM CPD 300, Wien, Austria), sputter-coated with carbon by means of a sputter-coating Nanotech Polaron-SEMPREP2 (Polaron Equipment Ltd., Watford, UK) and observed with a field emission scanning electron microscope (FESEM Gemini, Carl Zeiss, Oberkochen, Germany). To analyze for tubules occlusion, five images were taken at 1500X magnification in each specimen. Two examiners were previously calibrated on FESEM raw images and definitions of "open" (O), "partially filled" (P), and "filled" tubules [28]. A blind testing was performed; examiners were unaware of the study groups. The average of the two assessments was calculated for each specimen. The percentage of total occluded tubules (%TOT) was measured by dividing the sum of "partially filled" (P), and "filled tubules" (F) by the total number of tubules in an image [(P) + (F)]/total number x 100. The effect of NPs in occluding dentinal tubules was analyzed by comparing mean %TOT attained for each experimental group. Other images at a higher magnification were taken to ascertain for interactions between dentin and NPs. Energy-dispersive analysis was also performed in selected points using an X-ray detector system (EDX Inca 300, Oxford Instruments, Oxford, UK) attached to the FESEM.

2.5. Statistical methods

Statistical analysis was performed for dentin permeability, nano-DMA and tubular occlusion evaluations with ANOVA, Student Newman Keuls multiple comparisons ($P<0.05$) and Student *t* tests ($P<0.01$).

3. Results

The total number of dentin tubules occluded were evaluated for each nanoparticles-treated cervical dentin group, and displayed on Table 1. Untreated dentin was free from debris and with ~88% of completely open dentinal tubules, at 24 h time point (Fig. 1SIa). Some partially (~12%) filled tubules appeared after 7 d of storage (Fig. 1SIb). D-NPs only were able to fill ~61% of dentinal tubules at 24h, but after 1 week ~75% of tubules were newly opened. 100% of filled tubules were shown in cervical dentin treated with un-doped NPs at 24 h time point (Fig. 2a). After 7 d storage (Figs. 2b, 2c), only ~10% of tubules remained opened. Tubules were 100% filled, in dentin treated with Ca-NPs at 24 h or treated with Zn-NPs after 7 d (Figs. 2d, 2e, 2f). On these surfaces, spectra from energy dispersive analysis are showing elemental composition of phosphorous (P) and calcium (Ca), as main components.

The reduction of dentinal fluid flow obtained for each group is shown in Figure 3. At 24 h time point, cervical dentin treated with both NPs and Ca-NPs obtained the highest reduction of DFF. At 7 d time point, dentin treated with both Zn-NPs and Ca-NPs attained the greatest reduction of DFF. When groups assessed at 24 h and 7 d were compared, a significant increase of DFF was observed in cervical dentin treated with un-doped NPs and D-NPs. Specimens treated with Zn-NPs diminished their DFF to approximately 10% after 7 d of storage, and dentin treated with Ca-NPs did not change DFF values during the study periods.

Intertubular dentin (ID) treated with un-doped NPs and Zn-NPs attained similar storage modulus (E') if assessed at 24 h of storage. Intertubular dentin surfaces treated with Ca-NPs achieved the lowest E' (Table 2). Peritubular dentin (PT) followed the same trend, both PD treated with D-NPs and Ca-NPs decreased their E' at 24 h time point, but without differences between then. After 7 d of storage time, E' decreased at both PD and ID treated with both D-NPs and Ca-NPs. Loss modulus (E'') assessed at 24 h of storage

time increased after 7 d when treating ID with Zn-NPs, but it did not change at PD (Table 2). After 7 d of storage time, all groups behaved similar at ID. At PD, dentin treated with Ca-NPs obtained the lowest E'' (Table 2).

Intertubular dentin (ID) treated with D-NPs and Ca-NPs attained the lowest complex modulus (E^*) assessed at 24 h of storage (Fig. 4a). Untreated dentin achieved the lowest δ values after 7 d of storage at ID (Figs. 2SIa, 4b). At PD treated with Ca-NPs, the lowest E^* values were obtained among groups. After 7 d of storage time, both ID and PD treated with D-NPs and Ca-NPs obtained lower E^* (Figs. 4a, 5a) when compared with the rest of the groups. After 7 d of storage time, E^* assessed at PD significantly augmented in all groups, except in D-NPs (Figs. 2SIb, 4a, 5b). At 7 d of storage, Tan delta (δ) obtained at both ID and PD achieved the highest values after treating the cervical dentin with D-NPs. Tan delta (δ) of surfaces treated with Zn-NPs, at 7 d, showed intermediate values (Fig. 5c).

4. Discussion

Nanoparticles based on Ca-NPs and Zn-NPs produced the highest percentage of total occluded dentinal tubules by induced calcium-phosphate precipitates, and an almost complete reduction of fluid flow through dentin.

Two main methods are reported in the literature for the *in vitro* evaluation of potential dentin desensitizing agents, SEM analysis of dentin surfaces and permeability testing [32]. Dentin tubules in untreated samples were mostly opened (Table 1), but some of them (~10%) might have some calcium-phosphate deposits (Figs. 1SIa and 1SIb). These scarce intratubular minerals are insufficient to retain the fluid flow (Fig. 3). Tubular occlusion is impaired in untreated samples or at those surfaces treated with D-NPs, after 7 d of storage (Table 1). Cervical dentin treated with D-NPs exhibited a majority of open

tubules and low reduction of dentinal fluid flow, after 7 d of storage (Fig. 3). Previous reports have stated that doxycycline may open dentinal tubules [17,33], Kaur and Sikri, 2013). Thereby, D-NPs gel to treat DH is not recommended. Dentin treated with un-doped NPs achieved an approximately 90% reduction of dentinal fluid flow, at 24 h of storage, but a ~55% decrease at 7 d time point (Fig. 3). The bulk of mineral formations only allowed a restricted display of the dentinal tubules (Figs. 2b, 2c). The presence of ~90 % of total occluded tubules (Table 1) expressed the advanced occlusion capability and the efficient remineralizing effect [7] of the un-doped NPs based-gel. In addition, the low reduction of fluid flow (Fig. 3) at 7 d time point discouraged this nanoparticle for treating DH. A reduction in the flow rate reflects the resistance of attained tubule occlusion [26].

When dentin was treated with Ca-NPs or Zn-NPs, the reduction of dentinal fluid flow at 7 d of storage attained similar values, close to ~90% (Fig. 3). This substantial effect on the reduction in the flow rate is associated with an increase in the percentage of total occluded tubules (100%) after 7 d through calcium-phosphate salts deposits, as it was confirmed after FESEM and EDX analysis (Figs 2e, 2f). Mineral tags with Ca and P were principally detected (Figs. 2e, 2f) occluding dentinal tubules. At cervical dentin treated with Ca-NPs after 7 d of storage, tubules are completely or partially filled by precipitated minerals (Table 1) (Fig. 2e), and intertubular dentin is entirely remineralized. Other effective compounds as calcium sodium phosphosilicates form hydroxycarbonate apatite [4] which showed high rates of solubility [7]. Calcium, potassium, and ferric oxalate have also been used to treat DH, but oxalate precipitates were removed or dissolved by saliva [27]. Nano-hydroxyapatite, which has been recently recommended for tubular occlusion, forms soluble compounds that impair its long term efficacy [34].

Therefore, Ca-NPs or Zn-NPs based-gels demonstrated a great ability for dentinal tubule occlusion and must be considered as a viable treatment for DH, as they occluded

dentinal tubules by inducing calcium-phosphate precipitation. Nevertheless, this remineralized cervical dentin requires the capacity to absorb mechanical shock waves in order to prevent crack propagation across the surface. The presence of microfractures in the cervical region is debated. Most of the studies that confirmed fractures in dentin due to non-axial loading were based on finite elements analysis, while experimental or clinical evidences of these fractures are absent or weak [35]. The presence of these cracks reinforces the assumption that they can facilitate the penetration of acids, which demineralizes the hydroxyapatite around it, producing not only fracture but also caries disease [35].

Considering that both the storage modulus (E') and the loss modulus (E'') are involved in the viscoelastic expression of the complex modulus (E*) and tan δ, only E^* and tan δ will be discussed. Nano-DMA results revealed that there is heterogeneity in the mechanical property distribution between peritubular and intertubular dentin. The complex modulus is a measure of the resistance of a material to dynamic deformation [36]. Low different modulus (E^*) regions were observed close to relatively high elastic modulus regions (Figs. 3SIa, 4, 5a, 5b). As a result, E^* differences between peritubular and intertubular dentin treated with Zn-NPs were higher (~2.36 fold) than when Ca-NPs were employed (~1.85 fold). Dentin surfaces treated with Zn-NPs and Ca-NPs showed a ~ 5 and 4.6 fold lower tan δ values at peritubular dentin than at intertubular dentin, respectively, after 7 d of storage time (Fig 5c). The lower tan δ, the greater the proportion of energy available in the system for recoil and/or failure [37]. In the present study, the highest tan δ values became potentially associated to intratubular mineral precipitation (Figs 4, 5c). At the 3-D contour map of the tan δ distribution in a specimen at the dentin surface treated with Zn-NPs at 7 d of storage time, it was observed that tan δ values of intertubular dentin was an approximately 80% higher than with those attained at

peritubular dentin (Fig. 3SIb, 4b). Zones and signs of energy concentration hardly appeared at the dentin surface treated with Ca-NPs (Fig. 6a), due to the homogeneity of viscoelastic properties. Ca-NPs application provoked the lowest mechanical properties at both 24 h and 7 d in peritubular and intertubular, which denotes poor functional or intrafibrillar remineralization [3], slowing down the active dentin remodeling, with decreased maturity and low mechanical properties [11]. This discouraged its indication for DH treatment, and Zn-NPs are preferred.

The storage modulus E' (also called dynamic stiffness) characterizes the ability to store energy by the sample during a cycle of loading [19], which is then available for elastic recoil. It also determines the capacity of the substrate to withstand the crack in the first place. E' for Ca-NPs is approximately 1/3 and 1/5 that of the untreated PD and ID, respectively, at 24h and 7 days, while the Zn-NPs lead E' that is very similar to the untreated dentin at 24 h and 7 days, respectively (Table 2) (Figs 4SIa, 4SIb). This poses an additional advantage for Zn-NPs application at cervical dentin. Occluded tubules may affect dentin mechanical properties. Unfilled tubules have shown microcracking if compared with filled tubules, which can act as uncracked-ligament bridging [38,39]. Precipitated minerals are also located at the peritubular-intertubular dentin limit. The topography mapping obtained by AFM confirmed the existence of a neat stick-slip image at the peritubular-intertubular dentin edge, in samples treated with Zn-NPs at 7 d time point (Fig. 6b). These stick-slip images and little rod-like minerals appeared at the dentin surface as bridge-like structures [40]. These bridges of slipped mineralized dentin might be influential in effectively resisting crack propagation leading to fracture [39], by nucleating minerals at micro and nano-scale damage zones. It is speculated that the stick-slips formation when Zn-NPs were applied on dentin depends on the presence of the Zn^{++} in the chemical formulation of the nanoparticle, which originated new crystals

precipitation. These mineral formations were observed as multiple rod-like figures surrounding the intratubular crystals and at peritubular dentin [11] (Fig. 6c). These formations were absent in samples treated with un-doped NPs (Fig. 6d).

There are some limitations to this experiment. As a 7 d study, does not reflect a long-term effect of NPs. The results of 3 or 6 months observations are desirable. Moreover, it is essential to evaluate whether Zn-NPs and Ca-NPs based-gels have the potential to effectively occlude the dentin tubules and remineralize the dentin surface being resistant to environmental acids under circumstances similar to oral conditions. Further *in vitro* studies should investigate the ability of these nano-gels to reduce fluid flow through dentinal tubules before and after an acid challenge and the ability of these nanoparticle to remineralize carious lesions. Clinical studies will also be required to demonstrate that the present promising laboratory studies can be translated into benefits for patients. Future research should also be aimed to morpho-physico-chemically characterize these treated surfaces through micro-XRD^2, transmission electron microscopy, X-ray micro-computed tomography and X-ray fluorescence microscopy studies.

5. Conclusions

Un-doped NPs and D-NPs based-gels were not recommended for dentin hypersensitivity treatment, as a high percent of the dentin tubules remained open and the hydraulic conductance was not reduced. Nanoparticles based on Ca-NPs and Zn-NPs showed a total occlusion of dentinal tubules by induced calcium-phosphate precipitation and an almost complete reduction of fluid flow. Moreover, Zn-NPs produced improvements of dentin mechanical properties, probably increasing remodeling and dentin mineralization. As a result, they might be considered as a viable treatment for

dentin hypersensitivity, after performing additional experimental tests to overcome the limitations of the present *in vitro* study.

Disclosure

The authors report no conflicts of interest in this work.

Acknowledgements

This work was supported by the Ministry of Economy and Competitiveness (MINECO) and European Regional Development Fund (FEDER) [Project MAT2017-85999-P]. The authors thank the technical support of PhD Inmaculada Cabello for sample preparation and manuscript edition.

References

[1] C. Xu, Y. Wang, Collagen cross linking increases its biodegradation resistance in wet dentin bonding, J. Adhes. Dent. 14 (2012) 11–18.

[2] K.T. Yoshizaki, L.F. Francisconi-Dos-Rios, M. a. P. Sobral, A.C.C. Aranha, F.M. Mendes, T. Scaramucci, Clinical features and factors associated with non-carious cervical lesions and dentin hypersensitivity, J. Oral Rehabil. 44 (2017) 112–118.

[3] J.H. Kinney, S.J. Marshall, G.W. Marshall, The mechanical properties of human dentin: a critical review and re-evaluation of the dental literature, Crit. Rev. Oral Biol. Med. 14 (2003) 13–29.

[4] A. Jena, G. Shashirekha, Comparison of efficacy of three different desensitizing agents for in-office relief of dentin hypersensitivity: A 4 weeks clinical study, J. Conserv. Dent. JCD. 18 (2015) 389–393.

[5] E. Lynch, D.S. Brauer, N. Karpukhina, D.G. Gillam, R.G. Hill, Multi-component bioactive glasses of varying fluoride content for treating dentin hypersensitivity, Dent. Mater. 28 (2012) 168–178.

[6] M.G. Gandolfi, F. Iacono, C. Pirani, C. Prati, The use of calcium-silicate cements to reduce dentine permeability, Arch. Oral Biol. 57 (2012) 1054–1061.

[7] Z. Wang, T. Jiang, S. Sauro, D.H. Pashley, M. Toledano, R. Osorio, S. Liang, W. Xing, Y. Sa, Y. Wang, The dentine remineralization activity of a desensitizing bioactive glass-containing toothpaste: an in vitro study, Aust. Dent. J. 56 (2011) 372–381.

[8] R.R. Morães, J.W. Garcia, N.D. Wilson, S.H. Lewis, M.D. Barros, B. Yang, C.S. Pfeifer, J.W. Stansbury, Improved dental adhesive formulations based on reactive nanogel additives, J. Dent. Res. 91 (2012) 179–184.

[9] R. Osorio, I. Cabello, A.L. Medina-Castillo, E. Osorio, M. Toledano, Zinc-modified nanopolymers improve the quality of resin-dentin bonded interfaces, Clin. Oral Investig. 20 (2016) 2411–2420.

[10] V.P. Thompson, T.F. Watson, G.W. Marshall, B.R.K. Blackman, J.W. Stansbury, L.S. Schadler, R.A. Pearson, R. Libanori, Outside-the-(cavity-prep)-box thinking, Adv. Dent. Res. 25 (2013) 24–32.

[11] M. Toledano, R. Osorio, E. Osorio, A.L. Medina-Castillo, M. Toledano-Osorio, F.S. Aguilera, Ions-modified nanoparticles affect functional remineralization and energy dissipation through the resin-dentin interface, J. Mech. Behav. Biomed. Mater. 68 (2017) 62–79.

[12] R. Osorio , E. Osorio, I. Cabello, M. Toledano, Zinc induces apatite and scholzite formation during dentin remineralization, Caries Res. 48 (2014) 276-290.

[13] D.H. Pashley, FR. Tay, C. Yiu, M. Hashimoto, L. Breschi, R.M. Carvalho, S. Ito, Collagen degradation by host-derived enzymes during aging, J Dent Res. 83 (2004) 216-221.

[14] R. Osorio, M. Yamauti, E. Osorio, M.E. Ruiz-Requena, D.H. Pashley, F.R. Tay, M. Toledano, Zinc reduces collagen degradation in demineralized human dentin explants, J. Dent. 39 (2011) 148–153.

[15] M.A.R. Buzalaf, S. Charone, L. Tjäderhane, Role of host-derived proteinases in dentine caries and erosion, Caries Res. 49 Suppl 1 (2015) 30–37.

[16] R. Chaturvedi, A.S. Gill, P. Sikri, Evaluation of the regenerative potential of 25% doxycycline-loaded biodegradable membrane vs biodegradable membrane alone in the treatment of human periodontal infrabony defects: a clinical and radiological study, Indian J. Dent. Res. 19 (2008) 116–123.

[17] U.M. Wikesjö, P.J. Baker, L.A. Christersson, R.J. Genco, R.M. Lyall, S. Hic, R.M. DiFlorio, V.P. Terranova, A biochemical approach to periodontal regeneration: tetracycline treatment conditions dentin surfaces, J. Periodontal Res. 21 (1986) 322–329.

[18] M. Toledano, F.S. Aguilera, E. Osorio, M.T. López-López, I. Cabello, M. Toledano-Osorio, R. Osorio, On modeling and nanoanalysis of caries-affected dentin surfaces restored with Zn-containing amalgam and in vitro oral function, Biointerphases. 10 (2015) 041004.

[19] C.M. Hayot, E. Forouzesh, A. Goel, Z. Avramova, J.A. Turner, Viscoelastic properties of cell walls of single living plant cells determined by dynamic nanoindentation, J. Exp. Bot. 63 (2012) 2525–2540.

[20] M.A. Meyers, K.K. Chawla, Mechanical Behavior of Materials, Prentice Hall, New Jersey, 1999, pp. 98-103.

[21] M. Toledano, E. Osorio, I. Cabello, F.S. Aguilera, M.T. López-López, M. Toledano-Osorio, R. Osorio, Nanoscopic dynamic mechanical analysis of resin-infiltrated dentine, under in vitro chewing and bruxism events, J. Mech. Behav. Biomed. Mater. 54 (2016) 33–47.

[22] T.M. Wilkinson, S. Zargari, M. Prasad, C.E. Packard, Optimizing nano-dynamic mechanical analysis for high-resolution, elastic modulus mapping in organic-rich shales, J. Mater. Sci. 50 (2015) 1041–1049.

[23] A.L. Medina-Castillo, J.F. Fernandez-Sanchez, A. Segura-Carretero, A. Fernandez-Gutierrez, Micrometer and Submicrometer Particles Prepared by Precipitation Polymerization: Thermodynamic Model and Experimental Evidence of the Relation between Flory's Parameter and Particle Size, Macromolecules. 43 (2010) 5804–5813.

[24] R. Osorio, C.A. Alfonso-Rodríguez, A.L. Medina-Castillo, M. Alaminos, M. Toledano, Bioactive Polymeric Nanoparticles for Periodontal Therapy, PloS One. 11 (2016) e0166217.

[25] M. Toledano-Osorio, J.P. Babu, R. Osorio, A.L. Medina-Castillo, F. García-Godoy, M. Toledano, Modified polymeric nanoparticles exert antibacterial activity against planktonic cultures of Porphyromonas gingivalis, Int Endod J (2018). In press.

[26] S.Y. Kim, E.J. Kim, D.S. Kim, I.B. Lee, The evaluation of dentinal tubule occlusion by desensitizing agents: a real-time measurement of dentinal fluid flow rate and scanning electron microscopy, Oper. Dent. 38 (2013) 419–428.

[27] S. Sauro, C.-Y. Lin, F.J. Bikker, G. Cama, P. Dubruel, J.M. Soria, A. D'Onofrio, D. Gillam, Di-Calcium Phosphate and Phytosphingosine as an Innovative Acid-Resistant Treatment to Occlude Dentine Tubules, Caries Res. 50 (2016) 303–309.

[28] S. Sauro, T.F. Watson, I. Thompson, Dentine desensitization induced by prophylactic and air-polishing procedures: an in vitro dentine permeability and confocal microscopy study, J. Dent. 38 (2010) 411–422.

[29] H. Ryou, E. Romberg, D.H. Pashley, F.R. Tay, D. Arola, Nanoscopic dynamic mechanical properties of intertubular and peritubular dentin, J. Mech. Behav. Biomed. Mater. 7 (2012) 3–16.

[30] D.H. Pashley, F.R. Tay, R.M. Carvalho, F.A. Rueggeberg, K.A. Agee, M. Carrilho, A. Donnelly, F. García-Godoy, From dry bonding to water-wet bonding to ethanol-wet bonding. A review of the interactions between dentin matrix and solvated resins using a macromodel of the hybrid layer, Am. J. Dent. 20 (2007) 7–20.

[31] L. Han, A.J. Grodzinsky, C. Ortiz, Nanomechanics of the cartilage extracellular matrix, Annu. Rev. Mater. Res. 41 (2011) 133–168.

[32] Y. Zhang, K. Agee, D.H. Pashley, E.L. Pashley, The effects of Pain-Free Desensitizer on dentine permeability and tubule occlusion over time, in vitro, J. Clin. Periodontol. 25 (1998) 884–891.

[33] K. Kaur, P. Sikri, Evaluation of the effect of allograft with doxycycline versus the allograft alone in the treatment of infrabony defects: A controlled clinical and radiographical study, Dent. Res. J. 10 (2013) 238–246.

[34] J. Yu, H. Yang, K. Li, H. Ren, J. Lei, C. Huang, Development of Epigallocatechin-3-gallate-Encapsulated Nanohydroxyapatite/Mesoporous Silica for Therapeutic Management of Dentin Surface, ACS Appl. Mater. Interfaces. 9 (2017) 25796–25807.

[35] N.M.S. Leal, J.L. Silva, M.I.M. Benigno, E.A. Bemerguy, J.B.C. Meira, R.Y. Ballester, How mechanical stresses modulate enamel demineralization in non-carious cervical lesions?, J. Mech. Behav. Biomed. Mater. 66 (2017) 50–57.

[36] H. Ryou, D.H. Pashley, F.R. Tay, D. Arola, A characterization of the mechanical behavior of resin-infiltrated dentin using nanoscopic Dynamic Mechanical Analysis, Dent. Mater. 29 (2013) 719–728.

[37] V. Gopalakrishnan, C.F. Zukoski, Delayed flow in thermo-reversible colloidal gels, J. Rheol. 51 (2007) 623–644.

[38] K.J. Koester, J.W. Ager, R.O. Ritchie, The effect of aging on crack-growth resistance and toughening mechanisms in human dentin, Biomaterials. 29 (2008) 1318–1328.

[39] Y. Shinno, T. Ishimoto, M. Saito, R. Uemura, M. Arino, K. Marumo, T. Nakano, M. Hayashi, Comprehensive analyses of how tubule occlusion and advanced glycation end-products diminish strength of aged dentin, Sci. Rep. 6 (2016) 19849.

[40] R. Agrawal, A. Nieto, H. Chen, M. Mora, A. Agarwal, Nanoscale damping characteristics of boron nitride nanotubes and carbon nanotubes reinforced polymer composites, ACS Appl. Mater. Interfaces. 5 (2013) 12052–12057.

Table 1. Percentage of tubular occlusion (%) attained at the different experimental groups. Similar letters indicate no differences between the applied treatments, after ANOVA and Student-Newman-Keuls multiple comparisons ($p<0.05$). * indicates differences between 24 h and 1 week storage time within the same treatment group after Student t test ($p<0.001$).

	24h				1w			
	O	P	F	TOT	O	P	F	TOT
Untreated	87.7	12.3	0	12.3A*	77.9	22.1	0	22.1a*
NPs	0	0	100	100 C*	9.8	20.3	69.9	90.2b*
D-NPs	38.6	0	61.4	61.4B*	75.3	9.6	15.1	24.7a*
Zn-NPs	36.7	11.2	52.1	63.3B*	0	0	100	100c*
Ca-NPs	0	0	100	100 C	0	4.8	95.2	100c

Abbreviations: NPs: nanoparticles, D-NPs: doxycycline nanoparticles, Zn-NPs: zinc nanoparticles, Ca-NPs: calcium nanoparticles, O: open tubules, P: partially filled tubules, F: filled tubules, TOT: total occluded tubules.

Table 2. Mean and standard deviation (SD) of storage (E') and loss (E'') modulus (GPa) attained for experimental surfaces after 24 h and 7 days of PBS storage.

		Untreated		NPs		D-NPs		Ca-NPs		Zn-NPs	
		24h	7d	24h	7d	24h	7d	24h	7d	24h	7d
SM(*E'*) (GPa) Mean (SD)	PD	144.05 (40.71) A*	295.88 (27.88) a	137.98 (47.16) A*	285.40 (26.4) a	62.01 (11.30) B	65.54 (12.72) b	45.68 (12.85) B*	93.86 (21.29) b	112.01 (39.42) AB*	300.76 (29.90) a
	ID	157.80 (57.41) A	124.93 (41.45) a	67.95 (16.25) B	123.61 (42.60) a	40.61 (5.61) C	32.52 (4.16) b	27.38 (6.32) D*	47.01 (10.60) b	162.97 (52.14) A	142.97 (48.71) a
LM(*E''*) (GPa) Mean (SD)	PD	7.34 (2.77) A*	12.83 (0.91) a	X	5.69 (1.74) b	2.91 (0.85) C	2.91 (0.5) c	0.79 (0.21) D*	1.59 (0.06) d	1.55 (0.32) E*	2.92 (0.91) c
	ID	9.04 (2.57) A*	3.22 (1.08) a	2.10 (0.34) B	2.54 (0.61) a	2.58 (0.81) B	2.94 (0.75) a	1.51 (0.31) B	2.47 (0.66) a	10.38 (3.24) A*	2.89 (0.91) a

Abbreviations: PBS: Phosphate-buffered saline; NPs: unloaded nanoparticles; Zn-NPs: zinc doped nanoparticles; D-NPs: doxycycline doped nanoparticles; Ca-NPs: calcium doped nanoparticles; PD: peritubular dentin; ID: intertubular dentin; SM: storage modulus; LM: loss modulus; SD: standard deviation; PBS: phosphate-buffered solution. X: negligible data. Same letters (capital for 24 h and lowercase for 7 d) indicate no significant differences ($p < 0.05$) between the different experimental groups at the same zone. * indicates significant differences between the different storage periods in the same treatment group and zone.

Figure 1

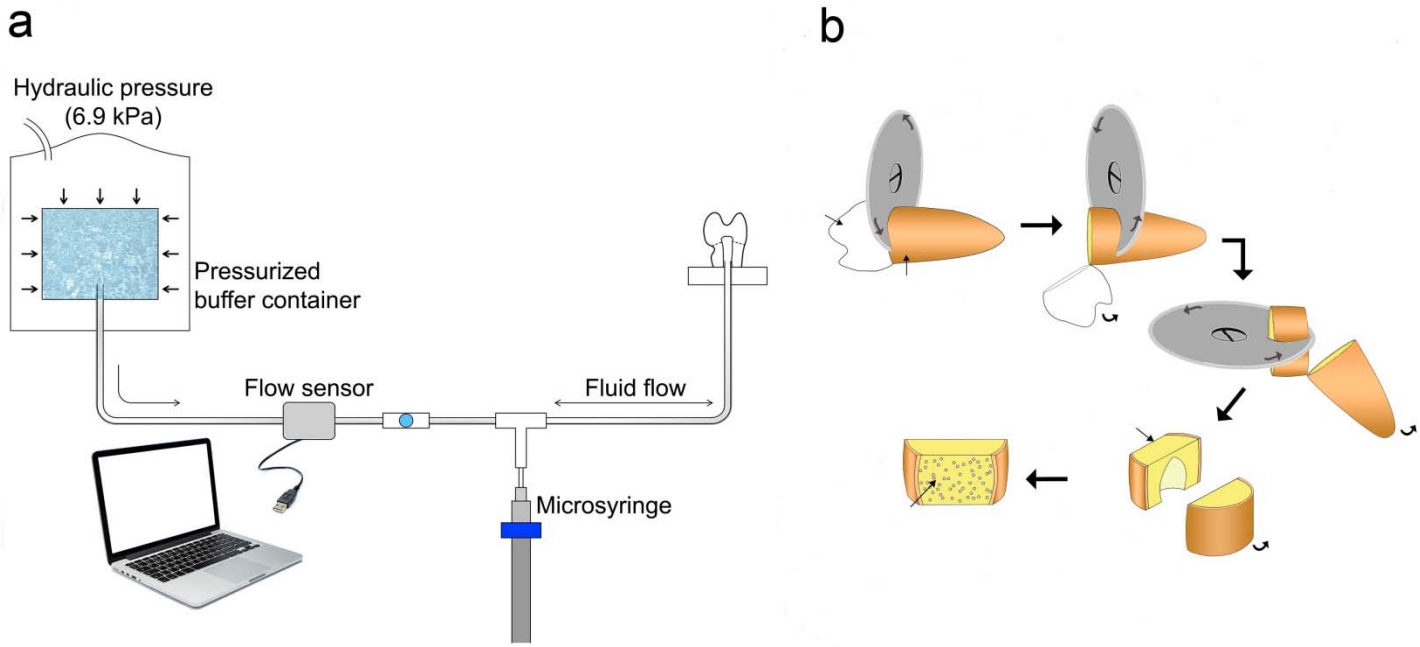

Figure 1. (**a**) Schematic illustration indicating how dentin permeability was measured. Specimens were connected to a hydraulic pressure device under a constant hydraulic pressure (6.9 kPa). The measurements of the changes in fluid volume were attained via a digital sensor. (**b**) Schematic representation of the **s**pecimen preparation. A tooth section was made to discard the crown (1), a longitudinal cut was also made to obtain two halves of the original specimen (2), dentin blocks were prepared by cutting below the cement-dentinal junction (3), surfaces were polished (4) to expose the cervical dentin.

Figure 2

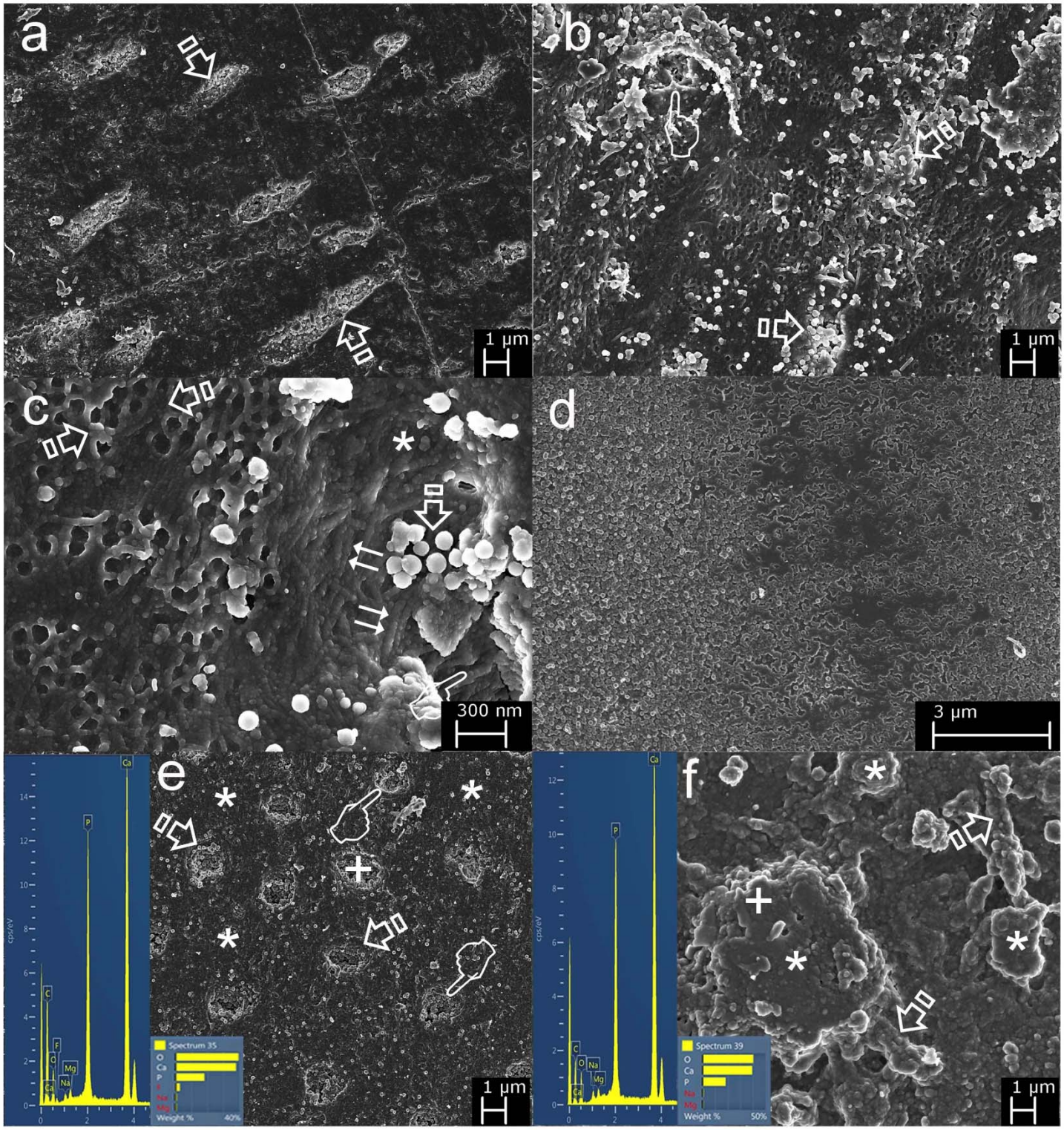

Figure 2. Representative FESEM topographic images of cervical dentin treated with un-doped NPs at 24 h (**a**), and 7 d (**b,c**) of storage. At 24 h time point, dentinal tubules were totally mineral filled (single arrows, at 2a and 2b). After 7 d of SBF storage, a net-shaped precipitated crystals appeared covering the intertubular and peritubular dentin. A first

layer of crystal nucleation was detected throughout the net (faced arrows, at 2c). Some partially filled tubules were shown (pointers, at 2b and 2c), with nucleated crystals coating the collagen fibrils and permitting the observation of the D-periodicity banding (67 nm) (double arrows, at 2c). Reduced areas of mineralization were also evident (asterisk, at 2c). NPs remained totally adhered to the remineralized collagen fibers (single arrow, at 2c). Dentin surface treated with Ca-NPs were observed at 24 h (**d**) and 7 d (**e**). At 24 h, a mineral deposition is completely covering the dentin surface. This substratum resulted totally mineralized and the mineral formations did not allow any display of the entrance of tubules. At 7 d time point, dentin tubules appeared completely (arrows, at 2e) or partially (pointers, at 2e) filled, and intertubular dentin appeared entirely remineralized (asterisks, at 2e). Cervical dentin treated with Zn-NPs is shown after 7 days of storage (**f**). The dentin surface exhibited multiple amorphous clumps of material scattered and grouped as dense network of buttons-like materials, rounding (asterisks, at 2f) or amorphous (arrows, at 2f). Tubules were occluded. Spectra from energy dispersive analysis, attained at zones 35 and 39, corresponding with the sign "+" at the images 2e and 2f, are showing elemental composition of phosphorous (P) and calcium (Ca), as main components.

Figure 3

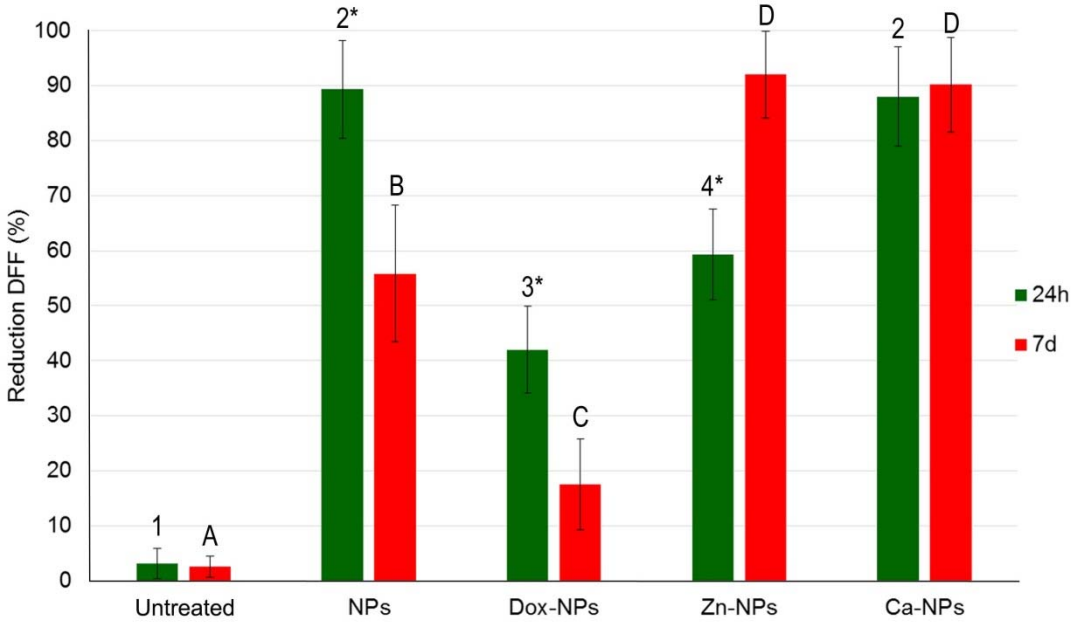

Figure 3: Reduction in dentinal fluid flow by the different NPs-based solutions. Similar numbers or letters indicate no significant differences among experimental groups ($p<0.05$), at 24 h and 7 d of storage, respectively. Asterisks mean significant differences between 24 h and 7 d storage time, within the same experimental group ($p<0.01$).

Figure 4

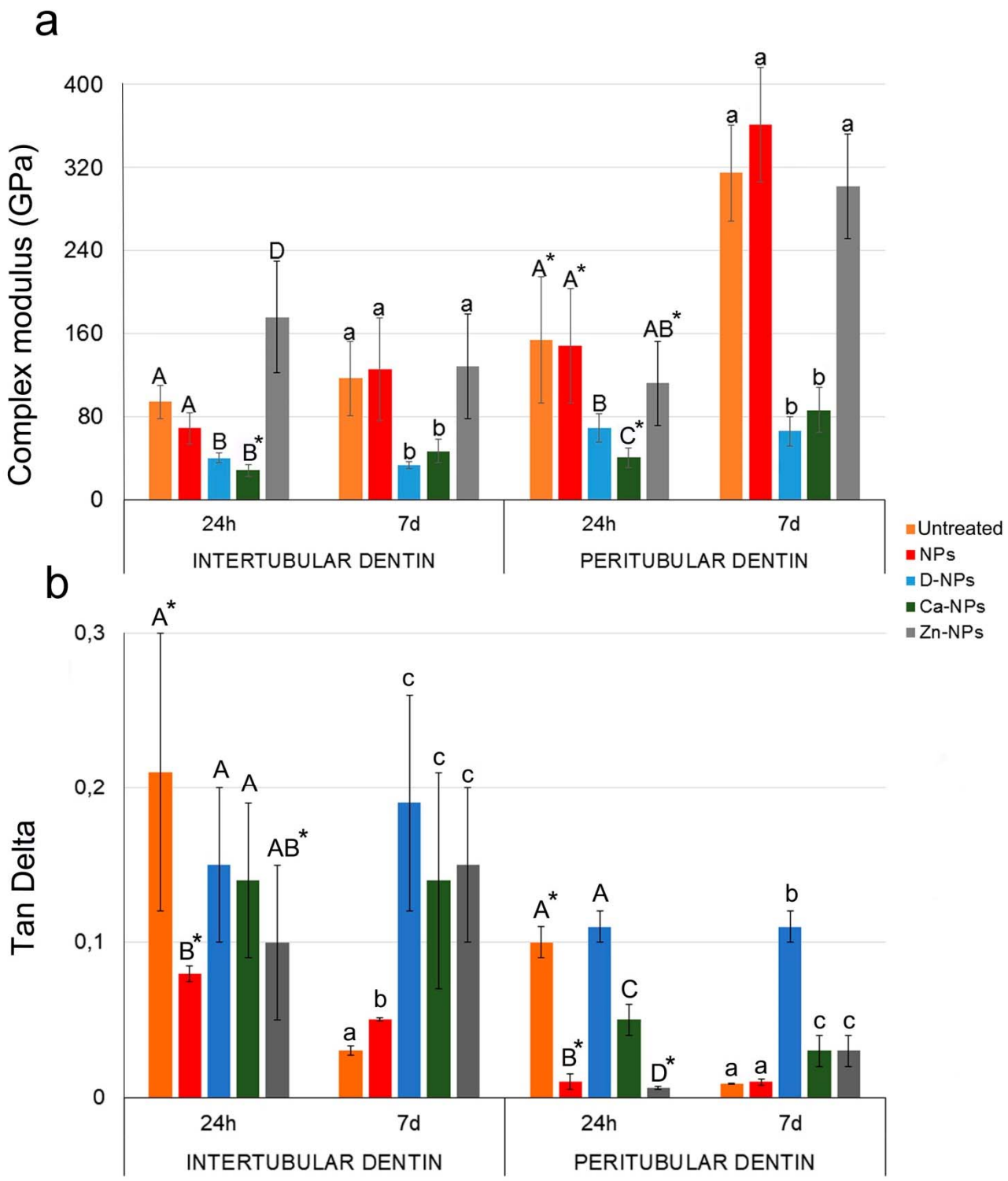

Figure 4. (**a**) Complex Modulus (GPa), at the different experimental dentin-treated surfaces. (**b**) Tan δ, at the different experimental dentin-treated surfaces. Similar capital and lowercase letters indicate no significant differences among experimental groups ($p<0.05$), at 24 h and 7 d of storage, respectively. Asterisks mean significant differences between 24 h and 7 d storage time, within the same experimental group ($p<0.01$).

Figure 5

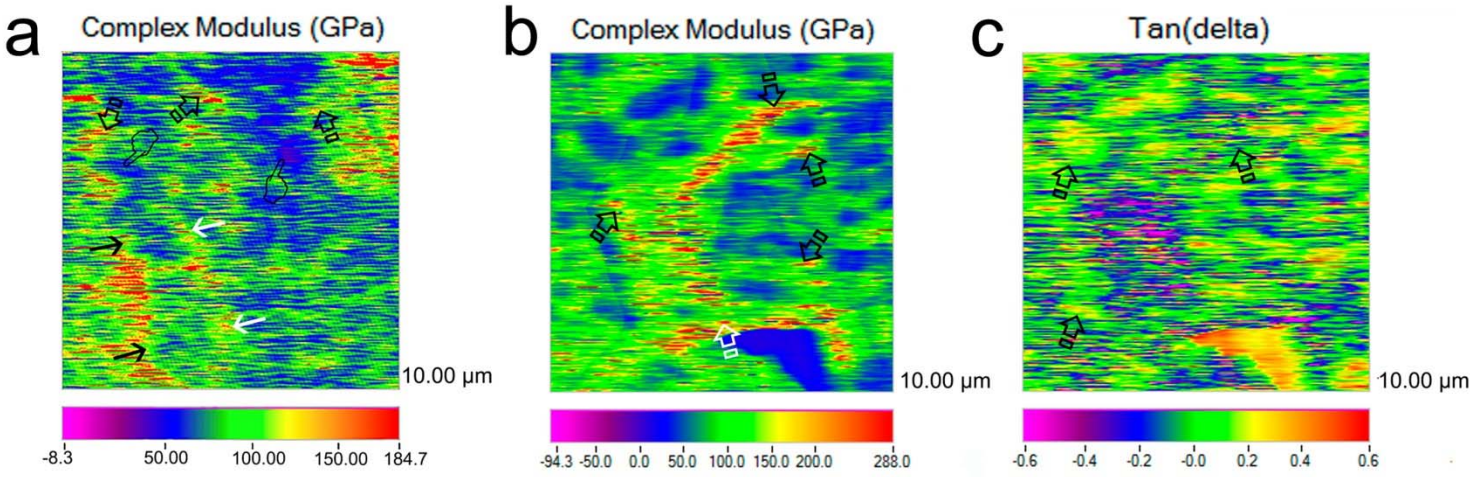

Figure 5. Scanning mode nano-DMA analysis of the map of the complex modulus (E^*) at the cervical dentin treated with Ca-NPs, obtained at 7 d (**a**) time point. In the color scheme shown, the red color corresponds to the highest value of the locally measured moduli, likely corresponding to the highest resistance to deformation of the peritubular dentin (arrows). E^* referred to intertubular dentin appears in bluish purple (pointers). The pixel data array at the mapping is organized according to E^* distribution that concurs with a clear delimitation between intertubular and peritubular dentin (faced arrows). Scanning mode nano-DMA analysis of the map of the complex modulus (E^*) at the cervical dentin treated with Zn-NPs, obtained at 7 d (**b**) time point. In the color scheme shown, the red color corresponds to the highest value of the locally measured moduli, potentially associated to E^* peritubular mineral precipitation. The red color represented the peritubular dentin. Peritubular dentin was associated with the red-staggered lines (arrows). Scanning mode nano-DMA analysis of the map of the tan δ at the cervical dentin treated with Zn-NPs, obtained at 7 d (**c**) time point. In the color scheme shown, the red color corresponds to the highest value of the locally tan δ value moduli, potentially associated to tan δ of intratubular mineral precipitation. The capacity for getting rid of the energy at peritubular dentin is represented by the blue-green diffused marks (arrows), at the mapping.

Figure 6

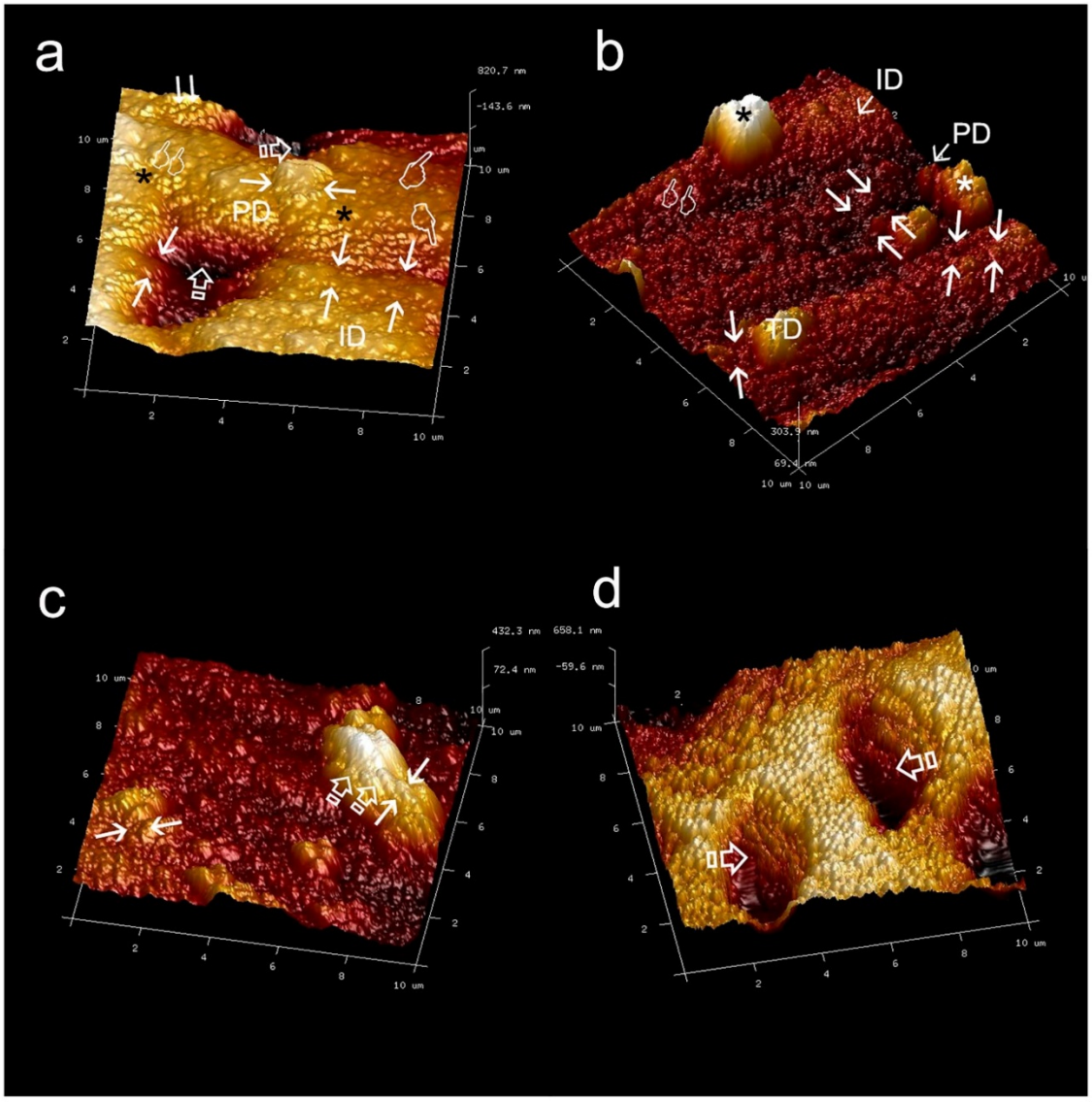

Figure 6. (**a**) Topography mapping of cervical dentin obtained by AFM after applying Ca-NPs, at 7 d time point. Some dentinal tubules appeared totally (pointers) or partially (single arrows) mineral filled. Strong processes of intertubular (ID) and peritubular (PD) dentin mineralization are observed (faced arrows). Morphologically, homogeneous transition between peritubular and intertubular dentin characterizes the dentin surface (asterisks). Zones-free from breakdown were observed anywhere. Nudes (double arrows) or mineral-integrated (double pointers) NPs were observed. (**b**) Topography mapping of cervical dentin obtained by AFM after applying Zn-NPs and 7 d time point. Peritubular (PD) and intertubular (ID) dentin mineralization is evident. Intratubular dentin (TD) is totally occluding the dentinal tubules (asterisks). Stick-slip images and little rod-like minerals (faced arrows), as bridge-like structures indicating sight of energy dissipation at the limits between both PD and ID are present. NPs were scarcely observed, most of them covered by a layer of mineral (double pointers). The crack deflection and branching, around the peritubular cuff, may be observed at the dentinal wall of an unfilled tubule (faced arrows) of dentin treated with Zn-NPs (**c**). Topography mapping of cervical dentin obtained by AFM after applying un-doped NPs (**d**) and 7 d time point. Some dentinal tubules appeared partially mineral filled (arrows).

Supplementary Material

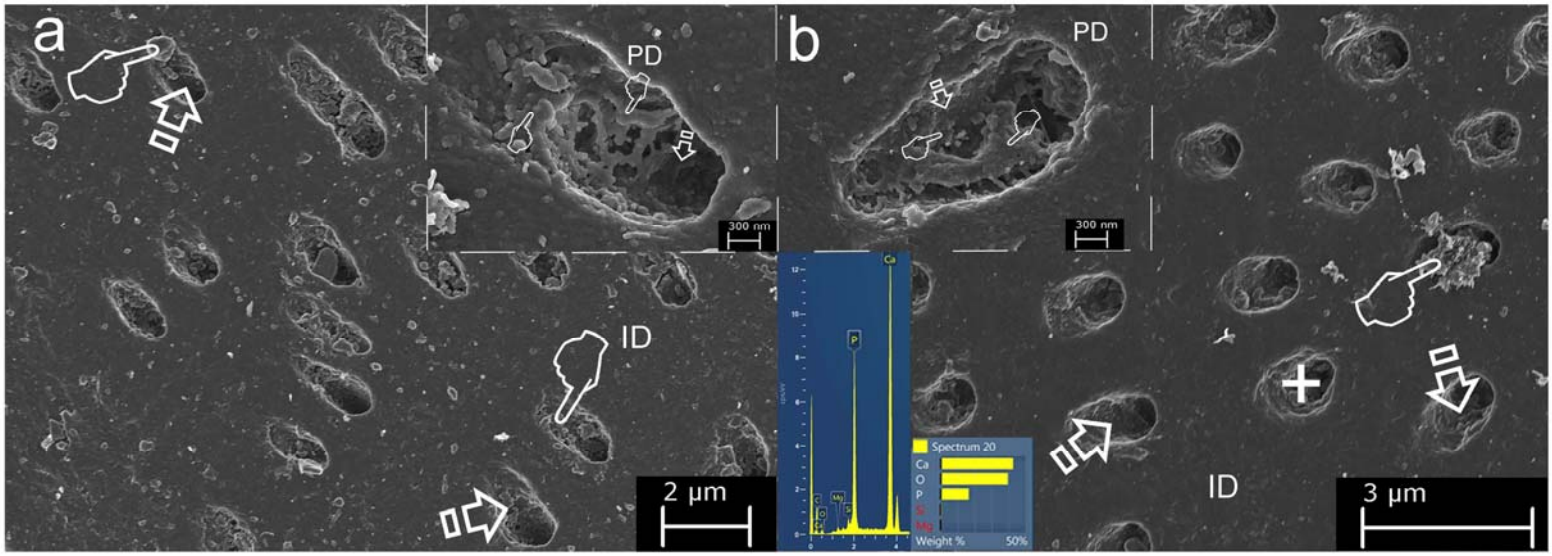

Figure 1SI. Representative FESEM topographic images of untreated cervical dentin stored in PBS for 24 h (**a**) or 7 d (**b**). ID, intertubular dentin. PD, peritubular dentin. Dentin tubules (arrows) were open, but partially occluded, with remains of smear plugs and mineral precipitates (pointers). Insets are showing the scarce tubular content to retain the fluid flow. Spectrum from energy dispersive analysis, attained at zone marked with "+" at image 1b, is showing elemental composition of phosphorous (P) and calcium (Ca).

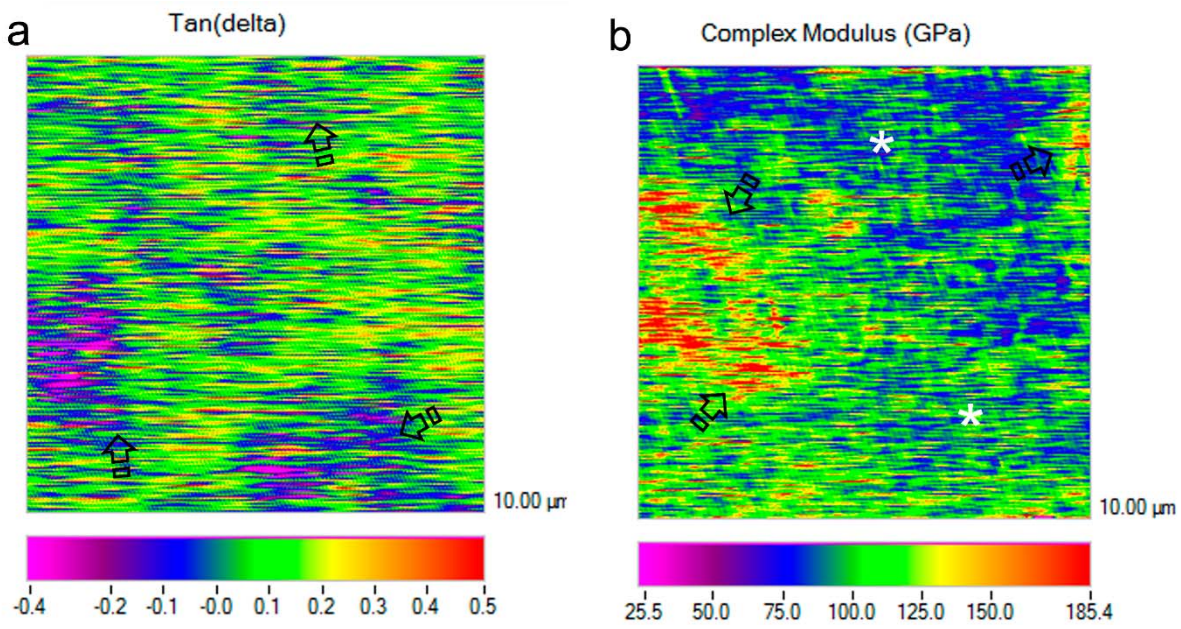

Figure 2SI. Scanning mode nano-DMA analysis of the map of the tan δ and complex modulus (E^*) at the untreated cervical dentin obtained at 7 d (**a**) and 24 h (**b**), respectively, stored in PBS. In the color scheme shown, the red color corresponds to the highest value

of the locally measured moduli, likely corresponding to the highest resistance to deformation (b) of the peritubular dentin. The intertubular dentin was represented by the greenish blue color (asterisks). In the color scheme shown, the red color corresponds to the highest value of the locally tan δ value moduli (a), potentially associated to tan δ of the intertubular dentin. The capacity for getting rid of the energy at peritubular dentin is represented by the greenish blue color (arrows) in samples assessed at 7 d, at the mapping.

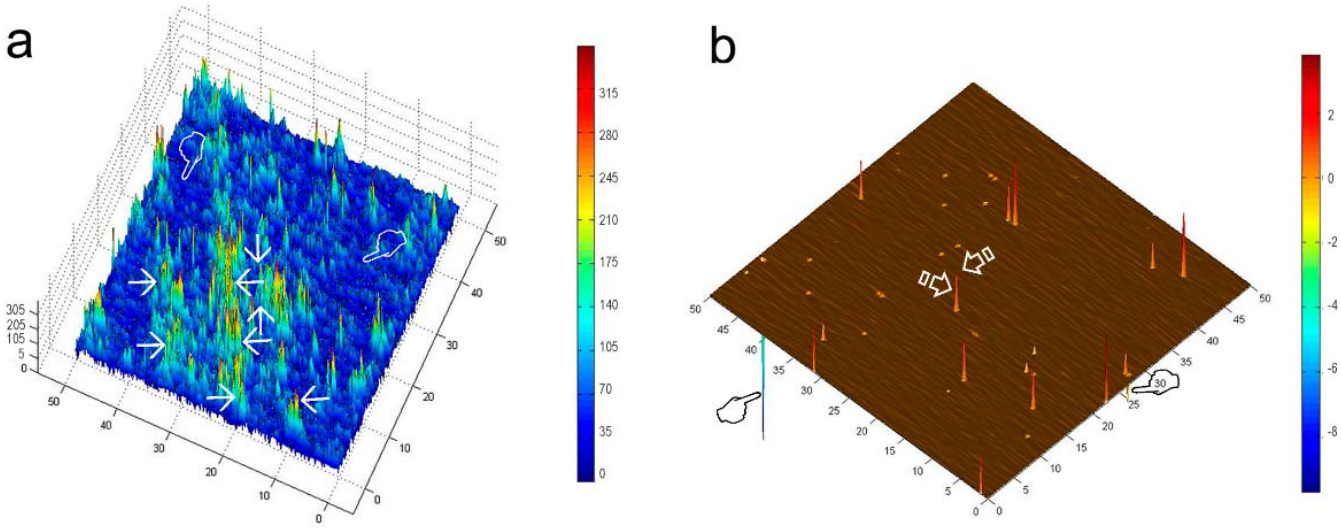

Figure 3SI. (**a)** 3-D contour map of the complex modulus (E^*) at the cervical dentin surface treated with Zn-NPs, 7d. In the color scheme shown, the red color corresponds to the highest value of the locally measured moduli. The mapping reflects regular and continuous rings of higher complex modulus (faced arrows), which correspond with the resistance to deformation of peritubular dentin (301.67 GPa). Extended areas of low values (pointers) may also be adverted, corresponding to the complex modulus of the intertubular dentin (128.06 GPa). (**b)** 3-D contour map of the tan δ distribution in a specimen at the cervical dentin surface treated with Zn-NPs, 7d time point. In the color scheme shown, the red color corresponds to the highest value of the locally measured moduli. At the dentin surface, tan δ ranged from 0.03 (peritubular dentin) to -7.8 (intertubular dentin). Peritubular dentin (arrows), produced an approximately 74% decrease of tan δ values in comparison with intertubular dentin (pointers), creating a zone of stress concentration at this junction.

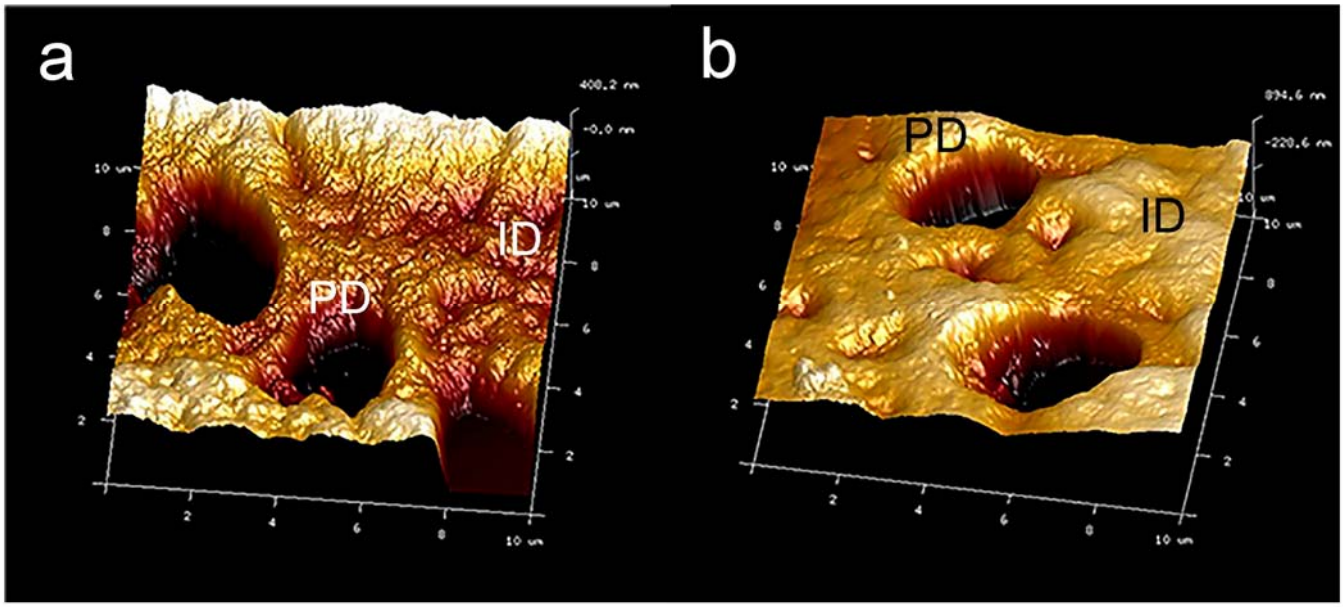

Figure 4SI. Topography mapping of untreated cervical dentin obtained by AFM after storing the sample for 24 h (**a**) and 7 d (**b**). Dentinal tubules appeared totally opened at both time points. Intertubular (ID) and peritubular (PD) dentin are well differentiated. Morphologically, homogeneous transition between peritubular and intertubular dentin characterizes the dentin surface at both mappings.